

# Complex impedance and conductivity of agar-based ion-conducting polymer electrolytes

A. C. Nwanya · C. I. Amaechi · A. E. Udounwa ·  
R. U. Osuji · M. Maaza · F. I. Ezema

Received: 28 October 2014 / Accepted: 31 December 2014 / Published online: 24 January 2015  
© Springer-Verlag Berlin Heidelberg 2015

**Abstract** Agar-based electrolyte standing films with different salts and weak acids as ion and proton conductors were prepared and characterized by X-ray diffraction, UV–visible spectrophotometry, photoluminescence emission spectroscopy and electrochemical impedance spectroscopy. The salts used are lithium perchlorate ( $\text{LiClO}_4$ ) and potassium perchlorate ( $\text{KClO}_4$ ), while the weak acids used are acetic acid ( $\text{CH}_3\text{COOH}$ ) and lactic acid ( $\text{C}_3\text{H}_6\text{O}_3$ ). The values of the ion conductivity obtained for the agar-based polymer films are  $6.54 \times 10^{-8}$ ,  $9.12 \times 10^{-8}$ ,  $3.53 \times 10^{-8}$ ,  $2.24 \times 10^{-8}$  S/cm for the agar/acetic acid, agar/lactic acid, agar/ $\text{LiClO}_4$  and agar/ $\text{KClO}_4$  polymer films, respectively. As a function of temperature, the ion conductivity exhibits

an Arrhenius behavior and the estimated activation energy is  $\approx 0.1$  eV for all the samples. The samples depicted high values of dielectric permittivity toward low frequencies which is due mostly to electrode polarization effect. The samples showed very high transparency (85–98 %) in the visible region, and this high transparency is one of the major requirements for application in electrochromic devices (ECD). The values of conductivity and activation energy obtained indicate that the electrolytes are good materials for application in ECD.

---

A. C. Nwanya (✉)  
National Centre for Energy Research and Development,  
University of Nigeria, Nsukka, Nigeria  
e-mail: chinweasum@yahoo.com

A. C. Nwanya · C. I. Amaechi · A. E. Udounwa ·  
R. U. Osuji · F. I. Ezema  
Department of Physics and Astronomy, University of Nigeria,  
Nsukka, Nigeria  
e-mail: ifeanyichukwuonline@yahoo.com

F. I. Ezema  
e-mail: fiezema@yahoo.com

R. U. Osuji · M. Maaza · F. I. Ezema  
Nanosciences African Network (NANOAFNET), iThemba  
LABS-National Research Foundation, 1 Old Faure Road,  
Somerset West 7129, P.O. Box 722, Somerset West,  
Western Cape Province, South Africa

R. U. Osuji · M. Maaza · F. I. Ezema  
UNESCO-UNISA Africa Chair in Nanosciences/  
Nanotechnology, College of Graduate Studies, University of  
South Africa (UNISA), Muckleneuk Ridge,  
P.O. Box 392, Pretoria, South Africa

## List of symbols

$\sigma$	Conductivity
$\sigma_0$	Constant related to the conductivity at 0 K
$E_a$	Activation energy
$K$	Boltzmann's constant
$T$	Temperature
$l$	Electrode separation
$R_b$	Bulk resistance
$A$	Area between the electrolyte and electrode
$C_b$	Bulk capacitance
$R_1$	Blocking interface resistance
$C_{PE}$	Constant phase element
$\varepsilon_r$	Complex permittivity
$\varepsilon'$	Real part of dielectric constant
$\varepsilon''$	Imaginary part of dielectric constant
$\varepsilon_0$	Permittivity of free space
$C$	Capacitance value with the sample
$C_o$	Capacitance without the sample
$\omega$	Angular frequency
$f$	Frequency
DSSC	Dye-sensitized solar cell
ECD	Electrochromic device
Tan $\delta$	Dissipation factor

## 1 Introduction

Polymer electrolyte generally refers to any macromolecular or supramolecular nano-aggregate doped with ionic and protonic sources, which gives a significant ion conductivity [1]. Natural polymer electrolytes in the form of conducting membranes or thin films play an important role in the field of materials science due to their interesting properties. They find extensive applications in the fabrication of devices such as electrochromic devices [2–5], dye-sensitized solar cells (DSSC) [6], sensors [7], photonics [8] and in situ EIS study of monuments [9]. In contrast to liquid electrolytes, solid-state ones have no or very limited problems with leakage or pressure-related distortions. Due to the environmental problems posed by synthetic and non-degradable polymers derived from fossil fuels, the use of natural and biodegradable polymers has been advocated by many scientists. Such natural polymers that have been used among others are polysaccharides like starch [10, 11], cellulose [12], agar [6, 13], gelatin [2, 14] and DNA from plants [5, 7]. Interest in natural polymers and its derivatives is largely due to their ability to be processed as films with good mechanical properties, adhesion to glass surfaces and metals as well as excellent transparency. Moreover, the great advantage is that these polymers are obtained from natural sources, are therefore biodegradable, and easily accessible and have a relatively low cost.

Polymer electrolytes based on natural molecules have shown comparable ion conduction with traditional polymer electrolyte based especially on polyethylene oxide (PEO). For example, Leones et al. [13] obtained conductivity of  $2.35 \times 10^{-5}$  S/cm at room temperature using agar, while Zoppi et al. [15, 16] obtained conductivity in the range of  $10^{-4}$  S/cm at 100 °C using electrolyte based on poly(-amide 6-*b*-ethylene oxide). In terms of stability, the natural polymer-based electrolyte is also comparable if not better than the traditional ones. Avellaneda et al. [17] showed that the starch-based electrolyte used for ECD gave a constant transmittance at both the bleached state and colored state for 2,000 cycles, but a 3 % increase in the transmittance at higher cycles of up to 25,000 was noted. Leones et al. [13] showed that the features of voltammograms of agar-based polymer electrolyte did not change after 200 cycles except for a small shift to more positive potential, while stability test done by Nei de Freitas et al. [17], using P(EO + EPI) polymer, showed a decay of 72 % in the cell (from 1.0 to 0.3 %) for the first 30 days. The stability of both types of polymer electrolytes can be improved with the removal of residual solvents [18]. The conduction in both types of electrolytes is basically the same and occurs through the exchange of ions between complexed sites. Some of the ions are weakly bound to site with electrons hence under

the influence of a dc electric field can easily be dissociated [19, 20].

Agar is a polysaccharide found in seaweed. In its natural state, agar occurs as carbohydrate structure of cell walls agarophytes algae, probably existing either in the form of calcium salts or a mixture of salts of calcium and magnesium. It is a complex mixture of polysaccharides composed of two main fractions: agarose, a neutral polymer, and agaropectin, a sulfated polymer chain [16]. Agarose (Fig. 1), the predominant component of agar, is a linear polymer, made up of the repeating monomeric unit of agarobiose. Agarobiose is a disaccharide made up of D-galactose and 3,6-anhydro-L-galactopyranose. This paper extensively describes the preparation and characterization of agar-based polymer electrolytes with different salts and proton conductors. In most of the reviewed literature, LiClO<sub>4</sub> and acetic acid are used as the ion and proton conductors. The inclusion of lactic acid and KClO<sub>4</sub> is to determine their applicability as proton and ion conductors in the agar-based polymer film membranes. X-ray diffraction (XRD) measurements were used to examine the structure of the films. The photoluminescence spectra of the films were obtained at room temperature using a Shimadzu RF-5300PC (Xe source) photoluminescence spectrometer. The dielectric properties and the conductivity studies were done by electrochemical impedance spectroscopy (EIS).

## 2 Experimental details

### 2.1 Polymer gel/film synthesis

All the chemicals used were of analytical grade, obtained from BDH and used without further purification. Polymeric electrolytes based on agar were synthesized by adding 0.5 g of agar to 30 ml of water plasticized with 0.5 g of glycerol and cross-linked with 0.5 g of formaldehyde. Different weights of lithium perchlorate (LiClO<sub>4</sub>) were added to the mixture, and the solution was stirred at 60 °C until complete dissolution of the solute. The ion

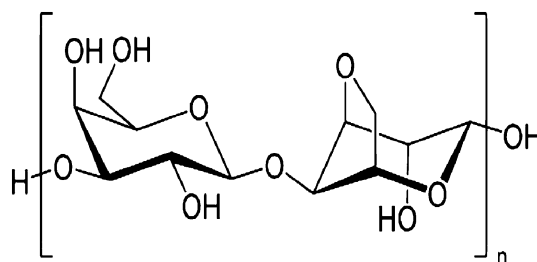


**Fig. 1** Structure of agarose

conductivity of the starting solution was measured using (Mettler Toledo SevenGo SG3) conductivity meter and then poured in a petri dish to form conductive films at room temperature. Samples of agar-based electrolyte using 0.05 M of different salts and weak acids (potassium perchlorate, acetic acid and lactic acid) were also developed and characterized.

The conductivity ( $\sigma$ ) of the electrolyte used in this study was first examined. This provides information on the mobility of the ions, their interaction with the solvent and on ion-pairing phenomena. Temperature dependence of ion conductivity can be described using Arrhenius equation:

$$\sigma(T) = \sigma_0 \exp(-E_a/KT) \tag{1}$$

where  $\sigma$  is conductivity,  $K$  is the Boltzmann constant,  $T$  is the absolute temperature,  $\sigma_0$  is a constant related to the conductivity at 0 K and  $E_a$  is the activation energy. Furthermore, the ion conductivity of the developed polymer film electrolyte was obtained from the Nyquist plot using the  $R_b$  values by employing the formula [21]:

$$\sigma = \frac{l}{R_b A} \tag{2}$$

where  $l$  is the electrode separation, i.e., the gap between electrodes or the thickness of the film,  $A$  is the contact area between the electrolyte film and the electrode and  $R_b$  is the bulk resistance. The complex permittivity ( $\epsilon_r$ ) or the dielectric constant of a system is defined by the following equation [22, 23]:

$$\epsilon_r = \epsilon' - j\epsilon'' = \epsilon' - j \frac{\sigma}{\omega \epsilon_0} \tag{3}$$

$$\epsilon' = \frac{C}{C_0} \tag{4}$$

$$C = \frac{1}{\omega R_b} \tag{5}$$

$$C_0 = \left[ 0.08854 \frac{A}{d} \right] (\text{pF})$$

where  $\epsilon'$  is the real part of dielectric constant,  $\epsilon''$  its imaginary part,  $\sigma$  is the conductivity,  $\omega$  the angular frequency ( $\omega = 2\pi f$ ),  $\epsilon_0$  is the permittivity of the free space,  $C$  and  $C_0$  are the capacitance values with and without sample, respectively,  $A$  is the area of the electrodes and  $d$  is the spacing between the electrodes or the film thickness.

Tan  $\delta$  is the dissipation factor and is defined as follows:

$$\tan \delta = \frac{\epsilon''}{\epsilon'} \tag{6}$$

$\epsilon''$  is also called the dielectric loss.

## 2.2 Characterizations

The structure of the films was examined using X-ray (Rigaku) diffractometer with power of 50 kV/50 mA and  $\text{CuK}\alpha$  irradiation in an angle range of  $20^\circ$ – $120^\circ$  at room temperature. The PL spectra were obtained by the photoluminescence spectrometer (ShimadzuRF-5301) at room temperature. The film was excited with monochromic light from a 150W xenon lamp passing through the diffraction grating, and a photomultiplier was used to monitor the multiplied luminescence signal. The transmittance spectrum was obtained using UV–vis spectrophotometer (Shimadzu UV 1800) in the wavelength range of 200–1,100 nm, while the surface morphology was obtained from high-resolution digital microscope fitted with digital camera (Shenzhen Gocamera). The EIS data of the formed films were obtained using a frequency response analyzer (FRA5087) and applying an excitation perturbation amplitude of 100 mV. Measurements were taken over 100 mHz–10 MHz frequency range in saturated KCl. Membranes were cut into 1.23 cm  $\times$  2.35 cm to fit the area of the platinum electrodes used for the measurement.

## 3 Results and discussion

### 3.1 Agar-based gel polymer characteristics

Figure 2 shows the variation of conductivity with the lithium salt for the agar electrolyte. The conductivity followed the typical trend of polymer–salt complexes [24]. It increased and attained a maximum (at 0.25 M) followed by a decrease. Conductivity increase is due to the increase in the charge carriers or mobile ions when the salt concentration is increased. These charge carriers include free ion and ion pairs. The quantity and mobility of charge carriers

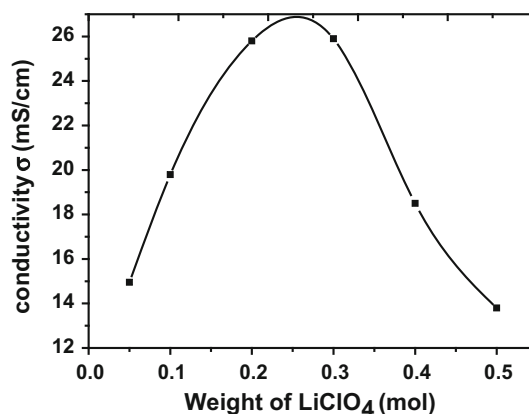


**Fig. 2** Influence of  $\text{LiClO}_4$  concentration on the conductivity of agar electrolyte

are the main factors that could affect the ion conductivity of polymer electrolytes as the charge of the mobile charge carriers is the same and is being ignored. By this principle, the ion conductivity is controlled strongly by the number of charge carriers at low concentration of salt and the mobility of ions is relatively unaffected.

However, beyond the optimum level, the ion conductivity is strongly dependent on the mobility of ions and the ion conduction pathway [25]. Beyond the optimum salt concentration, the distance between dissociated ions becomes too close to each other enabling them to recombine into neutral ion pairs, which do not contribute to conductivity. The ion pair model [26, 27] explains this. Moreover, solvents limit the solubility of these inorganic salts. If the salt added exceeds the solubility of salt in the polymer, it will separate out instead of dissolving in the polymer. Similar behavior is expected from the use of other salts and proton conductors.

The influence of temperature on the conductivity of the agar-based electrolyte with the salts and acids is shown in Fig. 3. As is apparent from Fig. 3, the ion conductivity increased linearly with inverse temperature, indicating an Arrhenius behavior. Therefore, Eq. 1 can be used to describe the conductivity–temperature behavior of the gel polymer electrolyte. Linear relations observed in the polymer electrolytes mean that there is neither phase transition in the polymer matrix nor domain formed by the addition of the salt and weak acids [27]. Linear variation of conductivity with inverse temperature is typical for polymers where hopping mechanism between the coordinating sites of the ionic and protonic charge species is predominant though other kinds of motion like segmental motion may be present [22, 28, 29]. Table 1 summarizes the line fit obtained for agar/LiClO<sub>4</sub>, agar/KClO<sub>4</sub>, agar/lactic acid and agar/acetic acid films, respectively.

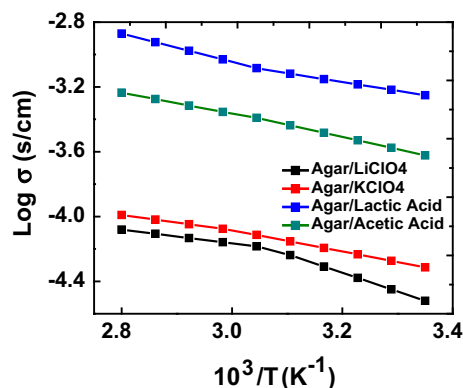


**Fig. 3** Temperature-dependence conductivity of the agar-based electrolyte

**Table 1** Line fit obtained for the temperature dependence of the agar polymer electrolytes

Electrolyte	Log $\sigma$	$R^2$
Agar/LiClO <sub>4</sub>	$-1.78803 - \frac{0.80255}{T}$	0.94675
Agar/KClO <sub>4</sub>	$-2.30504 - \frac{0.59721}{T}$	0.99461
Agar/lactic acid	$-0.97045 - \frac{0.68635}{T}$	0.98474
Agar/acetic acid	$-1.25839 - \frac{0.70359}{T}$	0.99792

$R^2$  is the coefficient of determination. The estimated activation energy is  $\approx 0.1$  eV for all the samples. The  $R^2$  value that is very close to unity indicates a strong relationship between conductivity and temperature. Figure 3 also indicates that the H<sup>+</sup> electrolyte shows more ion conductivity which agrees with the literature that in comparison with alkali metal salts, proton conductors are characterized by higher dynamics of ion transport [28]. The estimated activation energy of 0.1 eV obtained from the agar-based polymer electrolytes is slightly lower than 0.25 eV obtained by Leones et al. [12] using agar and some ionic liquids which they applied in ECD with the configurations glass/ITO/WO<sub>3</sub>/electrolyte/CeO<sub>2</sub>-TiO<sub>2</sub>/ITO/glass and got a good optical density. Raphael et al. [28] obtained values of activation energy in the range of 0.35–0.51 eV using agar and different percent weights of acetic acid. The lower activation energy is most probably due to the lower molarity values of the proton and ion conductors used as compared to the values used by other authors. The activation energy obtained is a comparable to what was obtained using other natural polymers like gelatin [2, 3, 22] and starch [30].

Table 2 shows the ion conductivity of the agar-based gel polymer electrolyte using 0.05 M of different salts and weak acids. The indicated temperature of measurement is the temperature below which the electrolyte gels and the solution conductivity could not be measured. The room temperature conductivity of the ion and proton sources without the polymer host is also indicated. It is seen from the table that the electrolyte conductivity varies with the ion and proton source. This is due to the differences in size and the number and mobility of the ions and protons in the different electrolytes. It has been shown that ion conductivity usually depends strongly on factors such as the types of cation and anion, salt concentration, temperature, etc. This dependence gives information on the specific interaction between the salt and the polymer matrix. For instance, lithium perchlorate and potassium perchlorate gave higher solution ion conductivity, but the conductivity of the developed polymer films as shown in Sect. 3.6 is lower indicating that the polymer cages these ions more than the protons when developed into a film.

**Table 2** Ion conductivity of agar-based electrolyte using 0.05 M of different salts and weak acids

Salt/acid	Salt/acid conductivity (room temperature) (mS/cm)	Agar electrolyte conductivity (mS/cm)	Temperature (°C)
Lactic acid	7.20	7.12	26.7
Potassium perchlorate	15.62	12.74	31.3
Acetic acid	5.26	2.56	31.9
Lithium perchlorate	14.5	8.59	29.0

### 3.2 X-ray diffraction studies

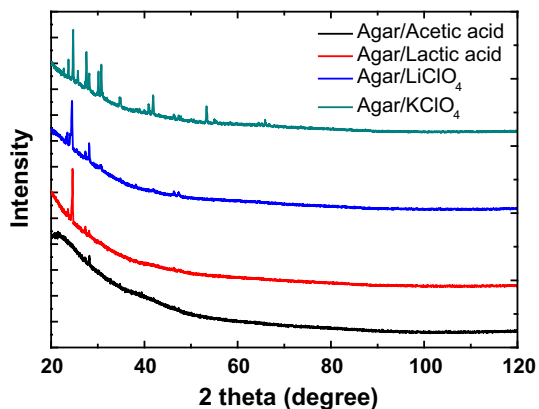
The X-ray diffraction patterns obtained for the agar-based polymer film electrolyte samples are shown in Fig. 4. The diffraction patterns show peaks in contrast to what is obtained in other ion-conducting membranes based on natural macromolecules [28, 31]. These increase in intensities indicate an increase in the local arrangement of polymer salt complexes-polymer backbone and consequently an increase in the crystallinity of the system.

### 3.3 Surface morphology

Figure 5 shows the surface morphology of the agar-based polymer electrolyte films. One can observe some inhomogeneity on the surface of the films with some scattered spots. The spots may be due to the encapsulation of some ions within the agar paste or due to ion pairing, whereby the free charge carriers became associated again [6, 13]. Those spots have the tendency to exhibit higher conductivity within the polymer films.

### 3.4 Photoluminescence studies

The photoluminescence emission spectra of all the samples recorded in the wavelength range of 779–1,700 nm are shown in Fig. 6. Photoluminescence spectra and their intensity dependencies can be used to determine the band gap energy and/or the wavelength of maximum gain, the impurity levels

**Fig. 4** XRD of the agar-based polymer films

and to investigate recombination mechanisms [32]. The spectral position of the peaks is almost the same for all the samples with two prominent peaks centered at 1,064 and 1,340 nm. The strong peak around 1.2 eV is due mostly to the strong interaction between the dopants (i.e., the salts and weak acids) with the agar polymer host, and this indicates high probability of radiative recombination of free charge carriers at the defects in polymer films. The broader peak centered around 1,340 nm could be assigned to the agar polymer host, and the acetic acid sample showed a higher intensity than the other samples at this region indicating that it had stronger interaction with the agar polymer host.

### 3.5 Optical properties

For applications in electrochemical devices, solid polymer electrolytes are developed with the aim of substituting the liquid ones. For most of these devices, a very important feature is their transparency. Hence, for applications in ECD and DSSC, solid polymer electrolyte is required to be transparent, especially in the visible region of the solar spectrum. While this transparency is easily obtained with liquid electrolytes, it is more difficult to realize with the solid ones [33]. Figure 7 shows the optical transmittance spectrum of the electrolytes in the range of 200–1,100 nm. It is observed that the transmittance of all the samples increased sharply with wavelength from 200 nm in the UV region to about 90–98 % in the visible region depending on the sample. The best transmittance values were obtained for the sample with LiClO<sub>4</sub> exhibiting transmittance of above 70 % over the whole wavelength region. For wavelengths higher than 650 nm, the transmission is practically constant and is optically well adapted for use in the devices. The transparency of the films is better than what was obtained using other natural polymers like agar [13, 28], starch [30] and DNA [33]. All the polymer film samples were obtained in the form of transparent and flexible membranes (Fig. 8), a clear advantage for their application in see-through and/or flexible devices like ECD and DSSC.

### 3.6 Impedance spectroscopy

The Nyquist plot for the agar-based polymer film electrolyte with different salts and weak acids at room

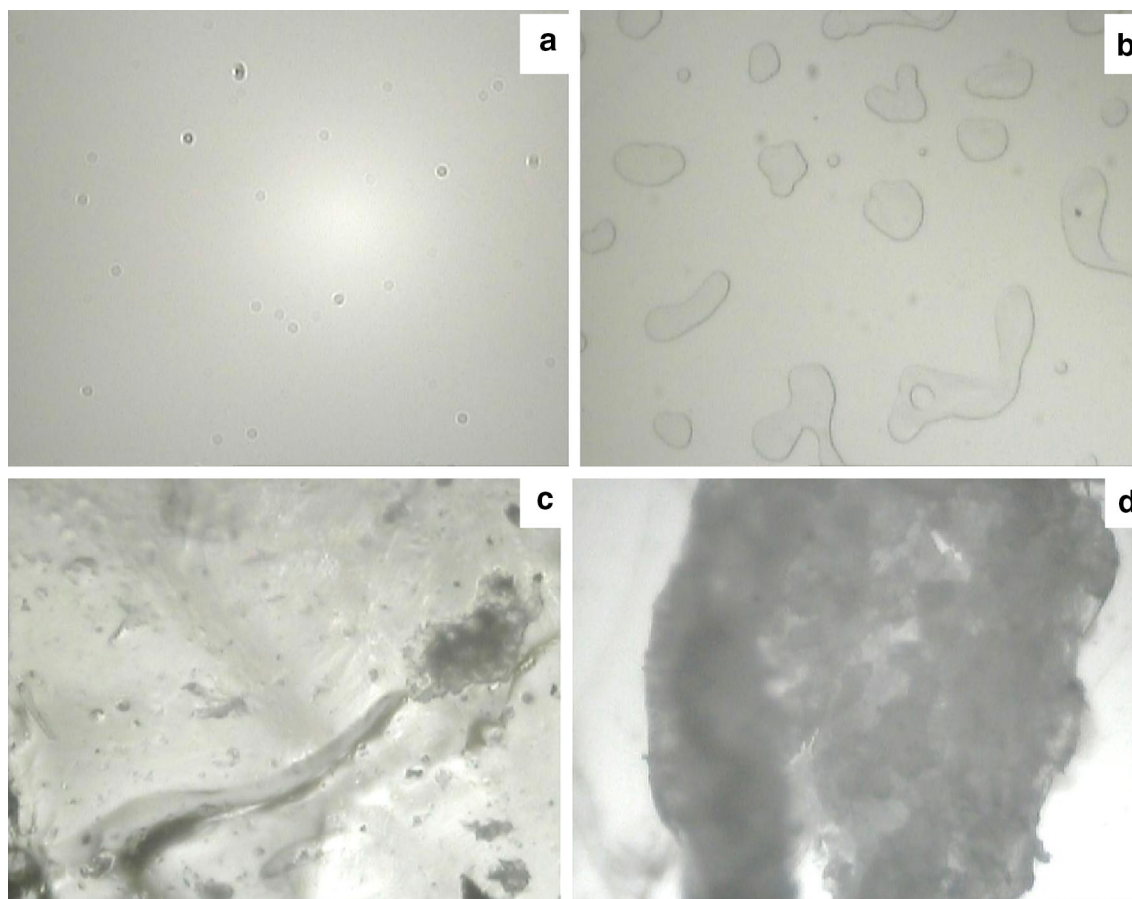


**Fig. 5** Surface morphology of the agar-based polymer films: **a** agar/KClO<sub>4</sub>, **b** agar/lactic acid, **c** agar/LiClO<sub>4</sub> and **d** agar/KClO<sub>4</sub> at a higher magnification

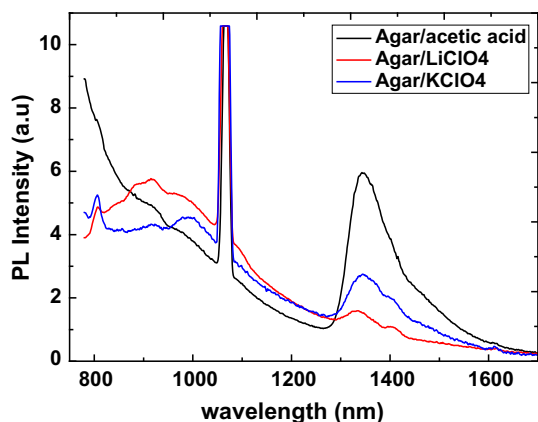


**Fig. 6** Photoluminescence spectra of the agar-based polymer films

temperature is shown in Fig. 9. The bulk resistance ( $R_b$ ) is given by the intercept of the semicircle with the real axis. The presence of incomplete semicircle suggests the appearance of a capacitive component at higher frequencies. The values of the ion conductivity obtained are  $6.54 \times 10^{-8}$ ,  $9.12 \times 10^{-8}$ ,  $3.53 \times 10^{-8}$  and  $2.24 \times$

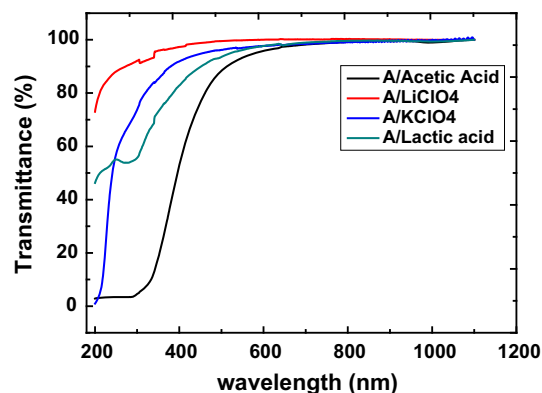


**Fig. 7** Transmittance spectrum of the polymer film electrolytes in the range of 200–1,100 nm

$10^{-8}$  S/cm for the agar/acetic acid, agar/lactic acid, agar/LiClO<sub>4</sub> and agar/KClO<sub>4</sub> polymer films, respectively. These values are low compared to what has been obtained using agar [13, 28], but the low conductivity values are due mostly to the very low molecular weight of the salts and weak acids used compared to what was used in the



Fig. 8 Standing film formed from the polymer electrolyte

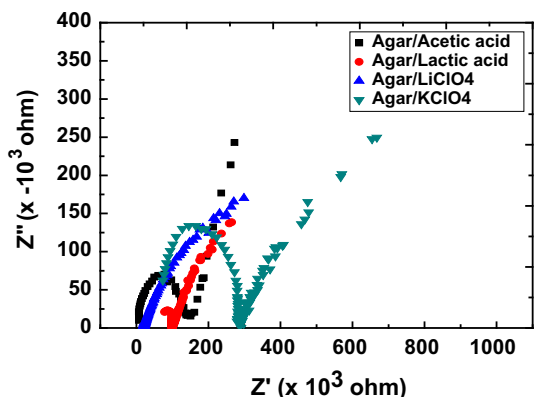


Fig. 9 Nyquist plot for the polymer films

reviewed literatures. The salts and weak acids gave comparative ion conductivity values, and this indicates that they can readily form polymer–salt complexes with the agar and the ions and protons could migrate through the polymer host comparatively.

Interpretation and quantification of the impedance spectrum requires understanding of the processes occurring in order to give the appropriate equivalent electric circuit model. The impedance of the polymer electrolyte film constitutes the bulk resistance,  $R_b$ , in parallel with the bulk membrane capacitance  $C_b$ . By placing the polymer film between the two electrodes, a blocking electrode–electrolyte interface is created. Each polymer–electrode interface is represented by a parallel combination of a capacitance, corresponding to the capacitance of the double layer, and a resistance, which models the resistance of the blocking interfaces,  $R_1$ . Faradaic charge cannot cross the interface; hence, the behavior of the electrode–electrolyte interface is mainly capacitive. The equivalent circuit model fitted with a software is shown in Fig. 10. It consists of  $R_1$  in series with a parallel connection of  $R_j$  (which represents the bulk resistance) and constant phase element  $C_{PE}$  (which represents a combination of the bulk capacitance and double-

layer capacitance). According to the equivalent circuit (Fig. 10), the impedance can be expressed as:

$$Z(\omega) = R_1 + \frac{R_j}{(\omega R_j C_{PE})^2 + 1} - i \frac{\omega R^2 C_{PE}}{\omega R_j (C_{PE})^2 + 1} \quad (7)$$

The plot of the  $|Z|$  and phase angle ( $\theta$ ) against frequency (Bode plot) is shown in Fig. 11. The figure indicates that all the studied samples show similar dependence of impedance on frequency. For the plot of  $|Z|$  against frequency, there is an increase in impedance toward the low frequencies and impedance relaxation toward the high frequencies. The impedance relaxation is characterized by occurrence of a dielectric peak between 5.5 and 6.5 MHz. The phase angle tends to zero through an intermediate frequency region similar to that where  $|Z|$  showed a frequency-independent plateau. This frequency range can be identified as that in which the impedance responses of these polymer films are basically resistive in nature [34]. The divergence of the phase angle from zero above and below this frequency region indicates the capacitive contribution from the polarization processes [35]. The Bode plot and the fitted result for the various samples are shown in Fig. 12. The figures show a good agreement between the experimental and impedance fitted data.

### 3.7 Dielectric analysis

The dielectric properties of the polymer thin film materials are used to determine the extent of the effectiveness of use as a medium in capacitors. Static dielectric constant also known as relative dielectric constant gives the ratio of stored electrical energy when a potential is applied relative to that of a vacuum [36]. It is used to express how easy it is for an applied electric field to induce a polarization in the material [37].

The plot of the  $\epsilon'$  versus  $\log f$  for the agar-based polymer electrolyte films containing different salts and weak acids at room temperature is shown in Fig. 13a. The dielectric constant of a polymeric material depends on interfacial, dipole, electronic as well as atomic polarizations. The atomic and electronic polarizations are instantaneous polarization components, the effect of which is seen only at high frequencies. The dipole or orientation polarization occurs due to the presence of polar groups in the material. The interfacial polarization arises due to heterogeneity,

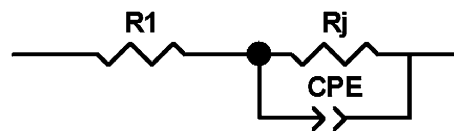


Fig. 10 Equivalent circuit model for the agar polymer electrolytes

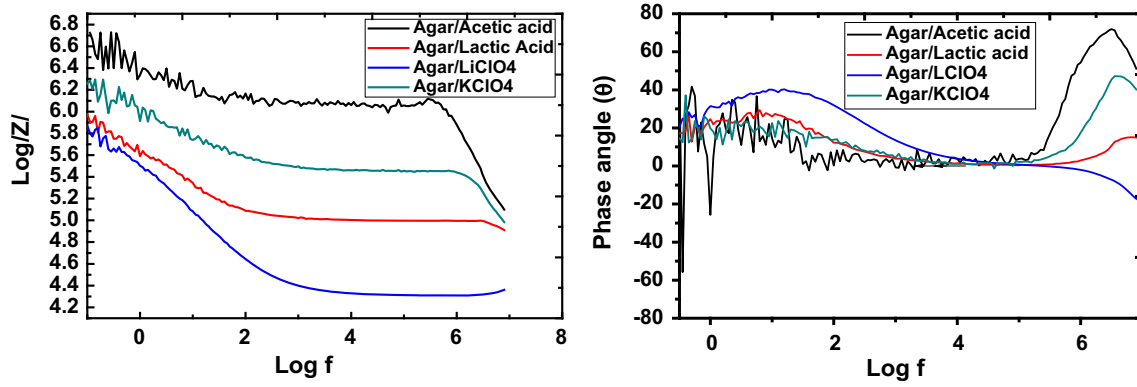


Fig. 11 Bode plot for the agar polymer films

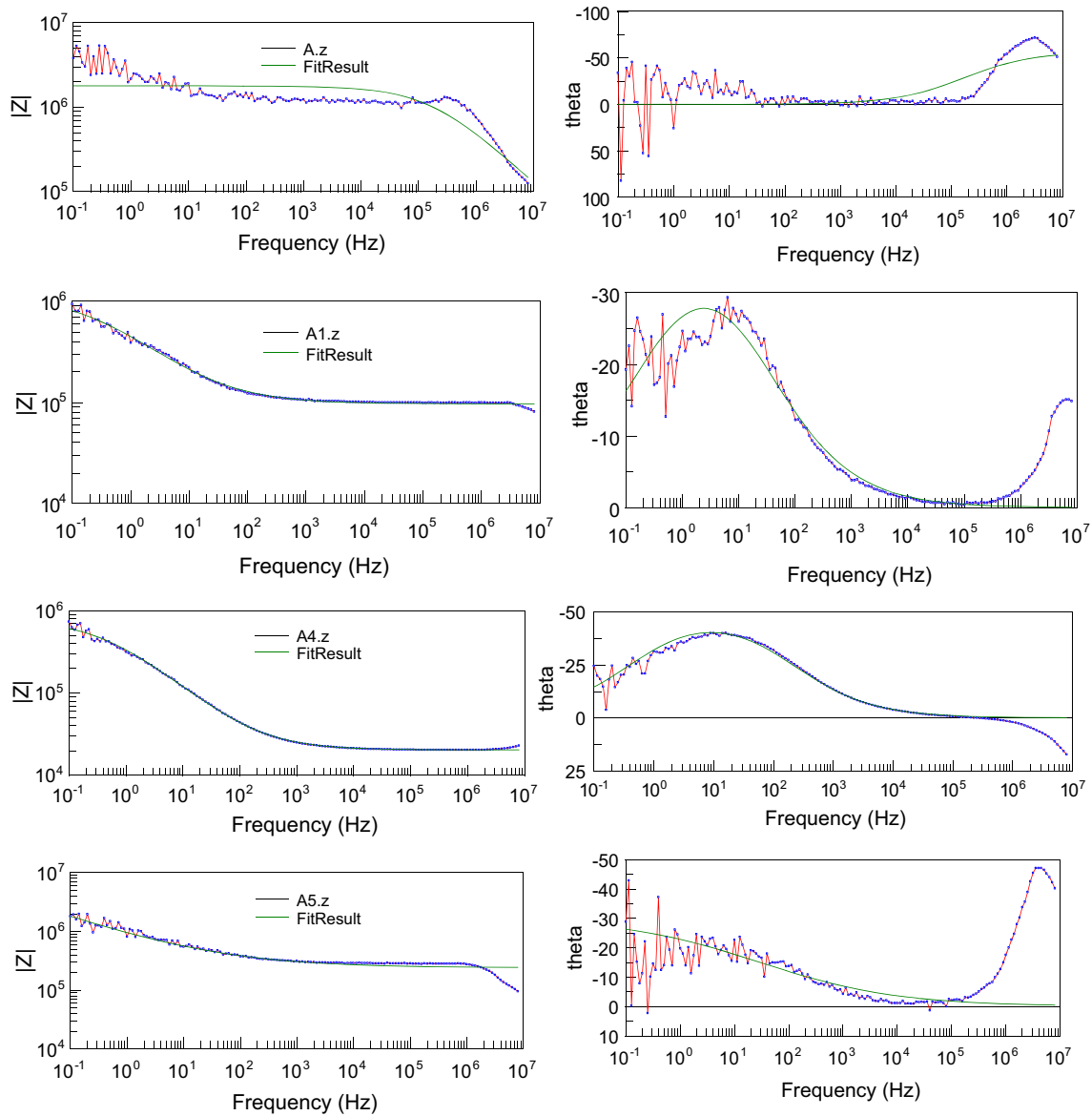
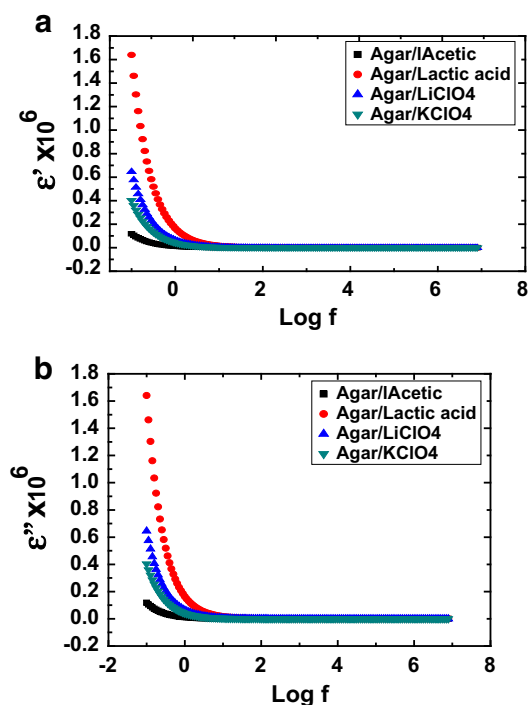


Fig. 12 Bode plot of experimental and equivalent circuit fitting (A.z = agar/acetic acetic, A1.z = agar/lactic acid, A4.z = agar/LiClO<sub>4</sub>, A5.z = agar/KClO<sub>4</sub>)





**Fig. 13** **a** Dielectric constant and **b** dielectric loss of the agar-based polymer film electrolyte as a function of frequency at room temperature for different salts and weak acids

which is highest at lower frequency [38]. Hence, the high values of dielectric permittivity exhibited by the samples toward low frequencies are due mostly to electrode polarization effect (dipolar polarization) which is a result of charge accumulation at the electrode–electrolyte interface [33, 39]. This leads to the inability of the mobile ions to cross the electrolyte–electrode interface and the eventual reduction in ionic current.

The plot of the dielectric loss  $\epsilon''$  versus  $\log f$  is shown in Fig. 13b. The behavior of dielectric loss with frequency is very much similar to  $\epsilon'$ , i.e., the highest dielectric loss is observed at low frequencies and its value decreases when the frequency increases. This behavior could be explained by the Maxwell–Wagner phenomena [32]. At high frequencies, the fast periodic reversal of the electric field leads to a decrease in the excess ion diffusion in the direction of the field so that the charge accumulation decreases and consequently leads to a decrease in the  $\epsilon''$  value [22].

#### 4 Conclusion

Polymer electrolytes based on agar and doped with some salts and weak acids have been prepared. The polymer film samples showed 85–98 % of transparency in the visible range depending on the sample. This high transparency in

the visible region is one the major requirements for application in ECD. The ion conductivity results as a function of temperature exhibited Arrhenius behavior, and the best values of activation energy were found to be 0.1 eV. The presence of incomplete semicircle in the Nyquist plot suggests the appearance of a capacitive component at higher frequencies. The values of the ion conductivity obtained are  $6.54 \times 10^{-8}$ ,  $9.12 \times 10^{-8}$ ,  $3.53 \times 10^{-8}$  and  $2.24 \times 10^{-8}$  S/cm for the agar/acetic acid, agar/lactic acid, agar/LiClO<sub>4</sub> and agar/KClO<sub>4</sub> polymer films, respectively. We established that lactic acid has a very high potential for use as proton conductor in polymer electrolytes given the high conductivity exhibited. The high transparency, the values of conductivity and activation energy obtained indicate that the electrolytes are good materials for application in electrochromic devices (ECD).

**Acknowledgments** The authors thank the US Army Research Laboratory–Broad Agency Announcement (BAA) for their financial support under the Contract Number W911NF12-1-0588 and W911NF12-1-0597.

#### References

- V.D. Noto, S. Lavina, G.A. Giffin, E. Negro, B. Scrosati, *Electrochim. Acta* **57**, 4–13 (2011)
- R. Leones, F. Sentanin, L.C. Rodrigues, R.A.S. Ferreira, I.M. Marrucho, J.M.S.S. Esperança, A. Pawlicka, L.D. Carlos, M.M. Silva, *Opt. Mater.* **35**(2), 187–195 (2012)
- M.M. Silva, P.C. Barbosa, L.C. Rodrigues, A. Gonçalves, C. Costa, E. Fortunato, *Opt. Mater.* **32**(6), 719–722 (2010)
- E. Lima, E. Raphael, F. Sentanin, L.C. Rodrigues, R.A.S. Ferreira, L.D. Carlos, M.M. Silva, A. Pawlicka, *Mater. Sci. Eng., B* **177**, 488–493 (2012)
- A. Pawlicka, A. Firmino, D. Vieira, F. Sentanin, J. G. Grote, F. Kajzar, in *Proceeding of the SPIE 7487, Optical Materials in Defence Systems Technology VI, 74870J* (September 24, 2009). doi:10.1117/12.835913
- S.S. Alias, A.A. Mohammed, *Ionics* **19**, 1185–1194 (2013)
- V. Velusamy, K. Arshak, O. Korostynska, K. Oliwa, C. Adley, in *Proceedings of the SPIE*, vol. 7315, p. 731504-1
- I. Rau, J.G. Grote, F. Kajzar, A. Pawlicka, *C. R. Phys.* **13**(8), 853–864 (2012)
- E. Cano, A. Crespo, D. Lafuente, B.R. Barat, *Electrochem. Commun.* **41**, 16–19 (2014)
- A. Pawlicka, D.C. Dragunski, K.V. Guimaraes, *Mol. Cryst. Liq. Cryst.* **416**, 105–112 (2004)
- P. Ramasamy, *Ionics* **18**, 413–423 (2012)
- A. Rubler, K. Sakakibara, *Cellulose* **18**, 937–944 (2011)
- R. Leones, F. Sentanin, L.C. Rodrigues, I.M. Marrucho, J.M.S.S. Esperança, A. Pawlicka, M.M. Silva, *Express Polym. Lett.* **6**(12), 1007–10011 (2012)
- D.F. Viera, C.O. Avellanneda, *Mol. Cryst. Liq. Cryst.* **485**, 95–104 (2008)
- D.R. Lu, C.M. Xiao, S.J. Xu, *Express Polym. Lett.* **3**(6), 366 (2009)
- J. Jane, S. Lim, I. Paetau, K. Spence, S. Wang, *ACS Symp. Ser.* **575**, 92 (1994)
- Y. He, H. Liu, Y. Chen, Y. Tian, Z. Deng, S.H. Ko, T. Ye, C. Mao, *Microsc. Res. Tech.* **70**, 522 (2007)

18. G.H. Meeten, P. Navard, *Polymer* **24**(17), 815–819 (1983)
19. K. Nakane, T. Ogihara, N. Ogata, Y. Kurokawa, *J. Mater. Res.* **18**, 672–676 (2003)
20. M.A.S.A. Samir, F. Alloin, W. Gorecki, J.-Y. Sanchez, A. Dufresne, *J. Phys. Chem. B* **108**, 10845–10852 (2004)
21. M. Vasilopoulou, I. Raptis, P. Argitis, I. Aspiotis, D. Davazoglou, *Microelectron. Eng.* **83**, 1414 (2006)
22. C.O. Avellaneda, D.F. Vieira, A. Al-Kahlout, E.R. Leite, A. Pawlicka, M.A. Aegerter, *Electrochim. Acta* **53**(4), 1648–1654 (2007)
23. Jurling A., in *Impedance Analysis and Breakdown Voltage of Dielectric Materials* (2008). [www.physics.oregonstate.edu/~tate/TateLabWiki/lib/exe/fetch.php](http://www.physics.oregonstate.edu/~tate/TateLabWiki/lib/exe/fetch.php). Accessed 11/3/14
24. F.M. Gray, *Solid Polymer Electrolytes: Fundamentals of Technological Applications* (Wiley-VCH, London, 1991), pp. 83–93
25. S. Ramesh, C.-W. Liew, A. Arof, K. J. Non-Cryst. Solids **357**(21), 3654–3660 (2011)
26. R.A. Robinson, R.H. Stokes, *Electrolyte Solutions* (Butterworths, London, 1959)
27. Y. Wang, *Sol. Energy Mater. Sol. Cells* **93**(8), 1167 (2009)
28. E. Raphael, C.O. Avellaneda, B. Manzolli, A. Pawlicka, *Electrochim. Acta* **55**(4), 1455–1459 (2010)
29. D. Baril, C. Michot, M. Armand, *Solid State Ion.* **94**, 35 (1997)
30. R.F.M.S. Marcondes, P.S. D’Agostini, J. Ferreira, E.M. Giroto, A. Pawlicka, D.C. Dragunski, *Solid State Ion.* **181**(13–14), 586–591 (2010)
31. A. Pawlicka, F. Sentanin, A. Firmino, J.G. Grote, F. Kajzar, I. Rau, *Synth. Met.* **161**(21–22), 2329–2334 (2011)
32. X.T. Zhang, Y.C. Liu, J.Y. Zhang et al., *J. Cryst. Growth* **254**(1–2), 80–85 (2003)
33. A.M. Neagu, I.V. Ciuchi, L.P. Curecheriu, L. Mitoseriu, *J. Adv. Res. Phys.* **1**(1), 011006 (2010)
34. T. Soboleva, Z. Xie, Z. Shi, E. Tsang, T. Navessin, S. Holdcroft, *J. Electroanal. Chem.* **622**, 145–152 (2008)
35. J.R. MacDonald, *Impedance Spectroscopy: Emphasizing Solid Materials and Systems* (Wiley, New York, 1987)
36. A. Firmino, J.G. Grote, F. Kajzar, J.-C. M’Peko, A. Pawlicka, *J. Appl. Phys.* **110**, 033704 (2011). doi:[10.1063/1.3610951](https://doi.org/10.1063/1.3610951)
37. M. O’Rourke, N. Duffy, R. De Marco, I. Potter, *Membranes* **1**, 132–148 (2011). doi:[10.3390/membranes1020132](https://doi.org/10.3390/membranes1020132)
38. Jurling A., in *Impedance Analysis and Breakdown Voltage of Dielectric Materials* (2008). [www.physics.oregonstate.edu/~tate/TateLabWiki/lib/exe/fetch.php](http://www.physics.oregonstate.edu/~tate/TateLabWiki/lib/exe/fetch.php). Accessed 11/3/14
39. N.A. Archana, N. Chand, *Int. J. Eng. Sci. Technol.* **4**(2), 191–209 (2012)